ISSN 0023-1584, Kinetics and Catalysis, 2011, Vol. 52, No. 1, pp. 128–138. © Pleiades Publishing, Ltd., 2011.
Original Russian Text © P.E. Strizhak, A.I. Trypolskyi, G.R. Kosmambetova, O.Z. Didenko, T.N. Gurnyk, 2011, published in Kinetika i Kataliz, 2011, Vol. 52, No. 1, pp. 131–142.

VIII INTERNATIONAL CONFERENCE ON MECHANISMS OF CATALYTIC REACTIONS

Geometric and Electronic Approaches to Size Effects in Heterogeneous Catalysis

P. E. Strizhak, A. I. Trypolskyi, G. R. Kosmambetova, O. Z. Didenko, and T. N. Gurnyk

Pisarzhevskii Institute of Physical Chemistry, National Academy of Sciences of Ukraine, Kiev, Ukraine

e-mail: pstrizhak@hotmail.com

Received November 25, 2009

Abstract—The influence of electronic and geometric factors is considered in the context of the manifestation of size effects in heterogeneous catalytic oxidation and hydrogenation reactions. Both of the factors are interdependent; however, the electronic factor predominates with regard to small metal and metal oxide particles (smaller than 10 nm), for which the energies of electron transitions in an activated complex are size-dependent. Only the geometry of active component nanoparticles exerts the main effect on the catalytic properties of coarser particles. In this case, the geometric factor depends on the accessibility of the active surface to reactants. The probability of the occurrence of complex active centers including several surface atoms increases as the active component particles of a catalyst become larger. The efficiency of the approach proposed to study the activating effect of nanophase catalysts is demonstrated using the oxidation and hydrogenation reactions of carbon oxides and the hydrogenation of acetonitrile and acetone as examples.

DOI: 10.1134/S0023158411010186

INTRODUCTION

The nanosized particles of active metals and metal oxides are of continuous interest to scientists who deal with the problems of catalysis. A great number of monographs and reviews have been devoted to studies of the dependence of the catalytic activity of substances on their surface morphology and particle size [1–8]. At the early stages of the development of the theory of heterogeneous catalysis, attention has been focused on the effect of the structure and texture characteristics of a catalyst upon its activity rather than the chemical nature of the catalyst. Roginskii [2] believed that the energy required for the activation of reactant molecules is accumulated in nonequilibrium, as a rule, highly dispersed systems and the activity of a catalyst depends on the occurrence of various types of surface defects, which possess an excess free energy (supersaturation theory). According to Kobozev, the structural organization of a catalyst is the main factor affecting its activity. In accordance with the ensemble principle by Kobozev, only amorphous formations consisting of one or more atoms of an active substance exhibit catalytic activity, whereas the surface of large crystals is catalytically inert [3, 4].

As early as the late 1940s, Boreskov [1] initiated fundamental studies on the activating capacity of the highly dispersed crystallites of catalytically active elements and their structure defects; his pupils and followers continued these studies [7, 8]. The activation effect of a number of catalytically active substances depends on preparation and treatment procedures, which affect the amount of possible surface defects. It was found that, in a number of cases, the specific catalytic activity of a solid at a constant chemical composition is independent of the dispersity of the active component, the degree of crystallinity, and the preparation procedure. This made it possible to formulate the so-called Boreskov rule on a constant specific catalytic activity of substances. Deviations from this rule were also detected; they were related to different catalytic activities of individual crystal faces. Note that the above results were mainly obtained in the course of the adsorption measurements of the total surface areas of catalysts and, in some cases, the surface area of an active component on inert supports. The subsequent progress in the determination of relationships between the catalytic activity of a solid and its electronic structure and structure and size characteristics became possible as a result of the development of modern instrumental techniques for studying substances at macro- and microlevels: high-resolution electron microscopy, transmission electron microscopy (TEM), and atomic force microscopy, as well as spectroscopic, magnetic, electronic, and diffraction techniques.

Boudart [9] studied the dependence of specific catalytic activity on the dispersity of the catalyst and found that the rate of reactions increased several times as the particle size was decreased, although the Boreskov rule was obeyed in the majority of cases. These reactions were referred to as structure-sensitive, and the reactions inconsistent with this rule were referred to as structure-insensitive.

More recently, heterogeneous catalytic reactions were tentatively subdivided into four types [10]. For the reactions of the first type (structure-insensitive),

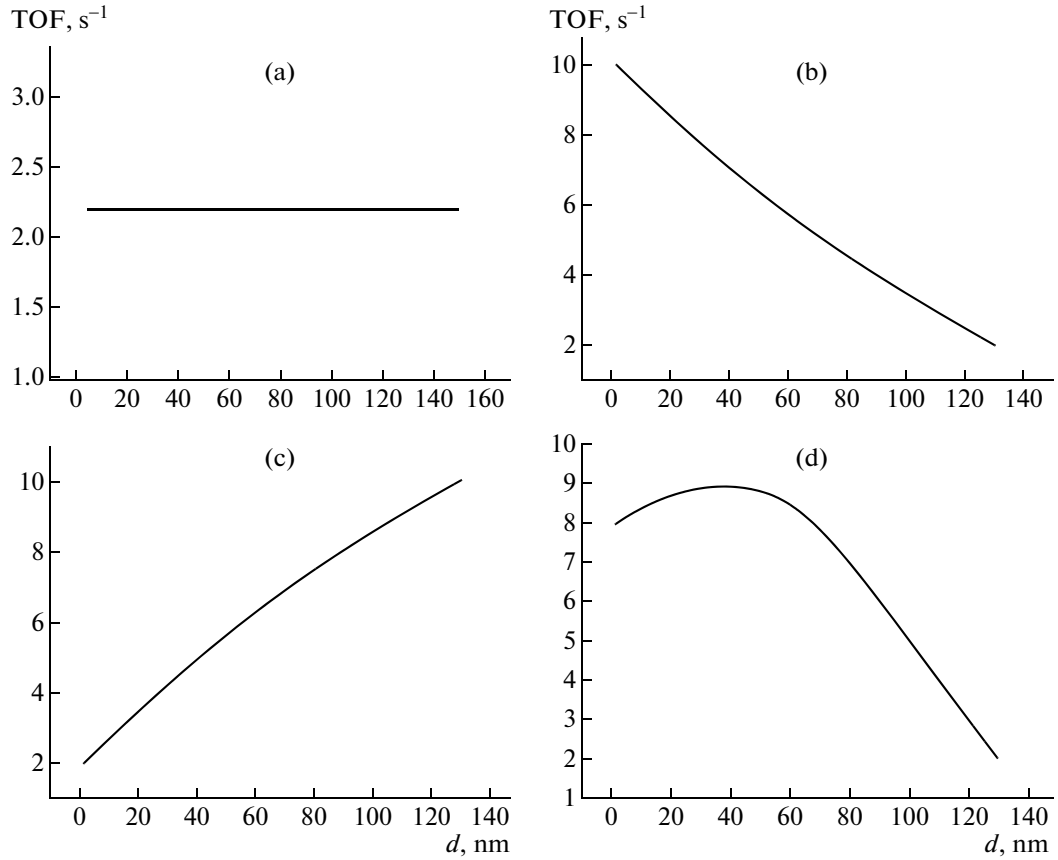

Fig. 1. Various types of the dependence of the turnover frequency of reaction on particle size: (a) structure-insensitive reaction, (b) structure-sensitive reaction with a positive size effect, (c) structure-sensitive reaction with a negative size effect, and (d) structure-sensitive reaction in which the turnover number passes through a maximum.

which obey the Boreskov rule, the turnover frequency (TOF) does not depend on particle size (Fig. 1a). In structure-sensitive reactions, TOF can either increase (Fig. 1b) with decreasing particle size (d) (i.e., small particles are more active than large ones (a positive size effect)) or decrease (Fig. 1c; a negative size effect). A variant when the TOF passes through a maximum can also occur; that is, medium-size particles exhibit the highest activity (Fig. 1d).

In accordance with the classical concepts of structure-sensitive reactions, the positive and negative size effects are due to different catalytic activities of centers arranged at crystal-lattice faces, edges, and corners, that is, the manifestation of a geometric factor [11, 12]. Correspondingly, information on the predominant localization of active centers can be obtained from the slope of the dependence of the logarithm of reaction rate on particle size. In the general case, if the slope is ≥ 1, ≥ 2, or about 3, active centers are arranged at the faces, edges, or corners of a crystal lattice. For the structure-sensitive reactions that obey the Boreskov rule, the slope is close to zero.

As an illustration, we can cite data on the catalytic activity of differently shaped platinum nanoparticles. The activity of structurally different platinum nanoparticles increases with the number of Pt atoms at the faces and corners of its crystal lattice in the following order: cubic structure < spherical structure < tetragonal structure [13].

The rates of the majority of heterogeneous catalytic reactions are described by increasing or descending nonlinear functions of particle size. A bell-shaped curve is observed rarely; as a rule, this shape is related to changes in the electronic structure of a catalyst when its particle size becomes smaller than 10 nm, that is, to the appearance of a so-called electronic factor. Here, it is reasonable to cite Bond [5], who wrote in 1985 that it is likely that the electronic properties of surface atoms themselves are more important than the coordination state; however, the presence of a specific group of atoms is required for some reactions; that is, these two factors should be balanced.

More recently, Bond [6] concluded that the assignment of size effects to the manifestation of geometric or electronic factors is tentative, and the question of whether the activity of metals depends on the electronic factor or the geometric structure has been actively discussed in the scientific literature. This is

similar to a choice of which leg, right or left, is more important; ultimately, they are interdependent. Note that the effect of the electronic factor on the catalytic properties of metals has been primarily considered in the context of electron density exchange between the outer *d* orbitals of the metal and the binding orbitals of adsorbed molecules [14]. In this case, the geometry of an adsorption complex is often a factor responsible for the activity of the catalytic system [8].

Nevertheless, for example, the question of which of the two factors under consideration is responsible for the catalytic properties of nanosized gold is still under active discussion. It has been considered for a long time that gold is inactive in catalytic reactions. First, this is due to its high caking capacity and difficulty to stabilize gold in a disperse state. The preparation of nanosized gold particles from colloid solutions [15–17] dramatically changed traditional concepts of the catalytic inertness of this metal because these particles exhibited unusually high activity and selectivity in redox reactions. It was found that nanocrystalline gold on various supports is highly active in the oxidation of CO and hydrocarbons and the reduction of nitrogen oxides, and it exhibits high selectivity in the catalytic process of the removal of carbon monoxide from hydrogen-containing gas mixtures by oxidation to CO_2 [17–20]. A characteristic feature of the above reactions is the nonmonotonic dependence of the catalytic activity of Au nanoparticles on particle diameter over the range of 2–5 nm [21]. Factors affecting the catalytic properties of gold nanoparticles in this range can be the following: the effect of a support and its chemical nature, charge transfer, the occurrence of a specific region at the active component–support interface, the coordinative unsaturation of surface gold atoms, and a quantum size effect due to the commensurability of the exciton wavelength and interplanar spacing in gold nanoparticles. An opinion has been expressed that the occurrence of surface low-coordination Au atoms, which exhibit enhanced adsorption properties toward CO and oxygen, plays a decisive role [21, 22]. To demonstrate this, the authors of the cited publications performed corresponding quantum-chemical calculations using the density functional theory. According to the results of these calculations, the geometric structure of active centers has a crucial effect on the electronic and derivative catalytic properties.

Goodman and coauthors [23–25] reported reliable evidence that the unusually high activity and selectivity of nanosized gold are due to the manifestation of quantum size effects. For example, the bell-shaped dependence of the activity in the reaction of CO oxidation on the size of Au nanoparticles can be explained by changes in the electronic properties of bilayer gold nanoclusters stabilized on the support surface. The observed change in the band gap in the region of 0.2–0.6 eV was due to metal transformation to an insulator at a particle size smaller than 3.5 nm. According to Goodman and coauthors [23–25], the manifestation of the catalytic properties of gold is related to this effect.

Palladium and silver nanoclusters and nanosized platinum films also exhibited unusually high activity due to a quantum size effect [26–29]. In the general case, the manifestation of quantum size effects in nanosystems are identified based on a band edge shift in the visible spectra to the blue region or broadening the band gap with decreasing particle size (as compared with coarsely crystalline substances).

Investigation of size effects in heterogeneous catalytic reactions on nanosized oxide systems is a challenging problem [28–32]. Stable metal oxide nanoparticles of the same size and shape are difficult to prepare. Therefore, the observed changes in catalyst activity cannot be unambiguously related to only one of the following possible reasons: quantum size effect, different coordinative unsaturation of metal atoms in oxides, support effect, or charge transfer from the support to the active component and vice versa. A comparison of the activities of bulk zinc, copper, and nickel oxides and their nanosized analogs in the reaction of methanol synthesis from CO and hydrogen demonstrated that the increased activity of ZnO (3.9 nm) and NiO (3.1 nm) nanoparticles was primarily due to a considerable increase in the specific surface areas of the samples, that is, the manifestation of a geometric factor [28].

Chen et al. [29] were the first to report the effect of an electronic factor on the catalytic activity of highly dispersed oxides (VO_x, MoO_x, WO_x, and NbO_x) supported on alumina, zirconia, and magnesia in the reactions of ethane and propane dehydrogenation. The reaction turnover frequency on these oxides, which are two-dimensional film domains, monotonically increased with decreasing energy of an absorption band edge determined from a blue shift in the electronic diffuse reflectance spectra of the samples. It was found that electronic transitions detected in the electronic diffuse reflectance spectra of metal oxides were mechanistically related to redox cycles in the process of the oxidative dehydrogenation of alkanes with the participation of the lattice oxygen of oxides. Note that the character of the observed dependence of the rate of hydrogenation on the energy of an absorption band edge was almost the same in all of the oxides regardless of the nature of the metal. Thus, differences in the electronic diffuse reflectance spectra of nanosized oxides, as compared with their bulk analogs, can serve as a characteristic of catalytic activity. This characteristic can play a key role in the study of the effect of an electronic factor on the catalytic properties of nanosized materials, including the size effect.

The aim of this work was to reveal the effects of electronic and geometric factors on the activity of heterogeneous catalysts under changes in the size of active component nanoparticles using oxidation and hydrogenation reactions as examples. The choice of a

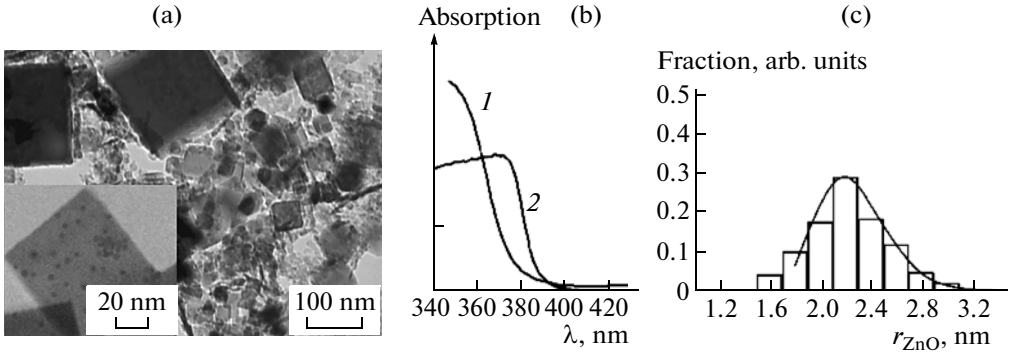

Fig. 2. Characteristics of the 1% ZnO/MgO catalyst: (a) TEM micrographs, (b) (*1*) electronic diffuse reflectance spectra, and (c) ZnO particle size distribution (the histogram and the curve were obtained based on TEM data and a diffuse reflectance spectrum, respectively). For comparison, (*2*) the electronic diffuse reflectance spectrum of a bulk sample of 1% ZnO–MgO, which was prepared by mixing the macrocrystalline powders of MgO and ZnO, is given.

catalyst was very important; the catalyst should be catalytically and optically active; it should have stable structure and valence to exclude effects caused by changes in these parameters, and it should be nanosized.

CARBON MONOXIDE OXIDATION REACTION

We used zinc oxide as a test material to study the effect of an electronic factor on catalytic properties. ZnO is an oxide on whose nanoparticles of size to 10 nm quantum size effects due to the discrete wave functions of electrons are observed. These effects manifest themselves in a broadening of the band gap and an increase in the redox potentials of the valence band and conduction band with decreasing size of nanoparticles [33, 34]. In heterogeneous catalysis, zinc oxide is used as an active component, support, and structure and texture modifier for copper-containing catalysts for the processes of organic synthesis and dehydrogenation, the catalytic purification of waste gases, and the preparation and purification of hydrogen and as a model material for studying the mechanisms of heterogeneous catalytic reactions [1].

Experimental

We prepared 1% ZnO/MgO catalysts with the average radius of zinc oxide nanoparticles from 2.00 to 2.30 nm. The nanoparticels were deposited onto a support from a colloid solution [35–38]. The average particle size was determined by analyzing particle size distributions found based on the electronic absorption spectra of ZnO nanoparticles in a colloid solution or the diffuse reflectance spectra of these particles supported on MgO. A band edge shift to the low-wavelength region suggests the presence of zinc oxide particles whose size lies within a so-called quantum range (<10 nm), where the band structure of zinc oxide is size-dependent, in the test samples. Electronic diffuse reflectance spectroscopy is a highly sensitive technique, which makes it possible to detect substances at concentrations of <1%. A comparison of the experimental results with TEM data supported the correctness of the use of electronic spectroscopy for evaluating the size of ZnO nanoparticles not only in a colloid solution but also upon supporting them onto a solid support (Fig. 2) [35, 38].

The band gap of ZnO nanoparticles was taken $E^* = 1240/\lambda_{1/2}$ ($\lambda_{1/2}$ is the wavelength at which the intensity of the electronic diffuse reflectance spectrum of 1% ZnO/MgO is 50% of the intensity of an exciton peak or shoulder) [39].

The average radius of ZnO nanoparticles was calculated from the particle size distribution found based on electronic diffuse reflectance spectra [35]:

$$n(r) \propto -\frac{dA/dr}{\frac{4}{3}\pi r^3},$$

where A is the absorption intensity, r is the nanoparticle radius, and $n(r)$ is the nanoparticle size distribution function. The radius of ZnO nanoparticles was determined from the electronic diffuse reflectance spectra using the effective mass model [38]:

$$E^{nano}(r) - E_g^{mass} = \frac{\hbar^2\pi^2}{2er^2}\left(\frac{1}{m_e^*} + \frac{1}{m_h^*}\right) - \frac{1.8e}{4\pi\varepsilon\varepsilon_0 r} - \frac{0.124e^3}{\hbar^2(4\pi\varepsilon\varepsilon_0)^2}\left(\frac{1}{m_e^*} + \frac{1}{m_h^*}\right)^{-1},$$

where E^{nano} is the exciton localization energy on a ZnO nanoparticle (eV); r is the radius of the ZnO nanoparticle (m); E_g^{mass} is the band gap of microcrystalline ZnO; $\hbar$ is the reduced Planck constant ($\hbar = h/2\pi = 1.055 \times 10^{-34}$ J s); m_e^* and m_h^* are the effective masses of an electron and a hole, respectively (for ZnO, $m_e^* = 0.26m_e$ and $m_h^* = 0.59m_e$); m_e is the mass of a free electron (9.11×10^{-31} kg); e is the charge of a

Table 1. Effect of the particle size of ZnO in 1% ZnO/MgO catalysts on their catalytic activity in CO oxidation and on the band gap

Catalyst	$\langle r \rangle \pm 0.05$, nm	E^*, eV	$W \times 10^7$, (mol CO) s^{-1} (g Cat)$^{-1}$	TOF $\times 10^3$, s^{-1}
K-1	2.01	3.49	0.8	2.6
K-2	2.03	3.48	0.8	2.6
K-3	2.05	3.47	0.9	2.6
K-4	2.12	3.43	1.1	3.3
K-5	2.16	3.40	4.2	9.5
K-6	2.20	3.41	10.3	13.1
K-7	2.23	3.40	2.2	10.0
K-8	2.25	3.42	1.5	9.2
K-9	2.26	3.39	0.9	1.5
K-10	2.29	3.39	1.5	1.8

free electron (1.602×10^{-19} J/eV); ε is the relative permittivity (for ZnO, it is 8.5); and ε_0 is the dielectric constant (8.854×10^{-12} F/m).

The catalytic activities of ZnO/MgO samples containing ZnO nanoparticles of various sizes were compared in terms of TOF, which was calculated from the specific rates of CO oxidation on a surface zinc atom at 320°C.

Results and Discussion

Table 1 summarizes data on the average radius of ZnO nanoparticles ($\langle r \rangle$), the band gap (E^*), and the turnover numbers calculated from the rates of CO oxidation (W) on catalysts K-1–K-10.

The catalytic activity of ZnO nanoparticles is a nonmonotonic function of band gap width and particle size. As can be seen in Fig. 3, catalyst K-6 ($\langle r \rangle$ = 2.20 ± 0.05 nm), whose band gap is $E^* \approx 3.41$ eV, exhibited a higher catalytic activity than samples with smaller and greater E^*. The highest values of TOF were observed on catalysts K-5–K-8 with band gaps of 3.40–3.42 eV, which contained ZnO nanoparticles with average radii of 2.16, 2.20, 2.23, and 2.25 nm, respectively. It is likely that the effects of changes in the amount of oxygen vacancies or the structure of nanoparticles can be ignored at these insignificant changes in the radius of ZnO. Note that the 1% ZnO/MgO catalysts prepared under different conditions but containing ZnO nanoparticles of the same size exhibited the same catalytic activity within the limits of experimental error. Thus, the catalytic activity of zinc oxide nanoparticles of size to 5 nm depends on an electronic factor, similarly to the activity of supported VO_x, MoO_x, WO_x, and NbO_x oxides in the dehydrogenation reactions of low-molecular-weight alkanes [29].

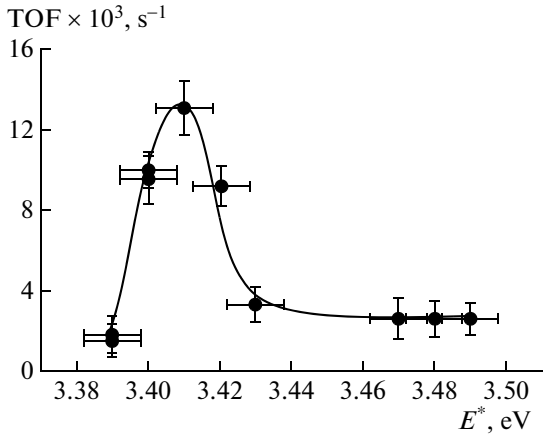

Fig. 3. Dependence of the turnover frequency in CO oxidation over zinc oxide nanoparticles on the band gap.

The particle size of an active component of a catalyst can affect not only the electronic state of active centers but also the energy of a catalytic process. The concentration of active centers and the probability of reactant adsorption on the planes of microcrystals also depend on the size of nanoparticles.

HYDROGENATION REACTIONS

Next, we consider an approach that allows us to take into account the effect of the particle size distribution of an active component of a supported catalyst on the preexponential factor of the rate constant of a heterogeneous catalytic reaction. The adequacy of the resulting theoretical dependences will be tested using the kinetics of hydrogenation of acetone, acetonitrile, carbon monoxide, and carbon dioxide in the presence of a number of transition metals on various supports as examples.

Table 2. Physicochemical and catalytic properties of various catalysts in acetone hydrogenation [40, 41]

Entry	Catalyst	S_0, m^2/(g metal)	d, nm	E_3, kJ/mol	$\ln k_{0(3)}$
1	Co/Al_2O_3	75	7.5	68	7.31
2	Ni/Al_2O_3	212	2.4	43	1.7×10^{-3}
3	Cu/Al_2O_3	165	3.4	58	4.3
4	Cu/Cr_2O_3	24	23	70	11.93
5	Ru/Al_2O_3	90	4.4	39	−0.21
6	Rh/Al_2O_3	163	2.5	17	−7.72
7	Ir/Al_2O_3	38.5	5.8	71	8.3
8	Pt/Al_2O_3	60	3.9	31	−1.68
9	Co	20	28.4	80	11.15

Experimental

The kinetics of hydrogenation of carbon oxides, acetonitrile, and acetone was studied at atmospheric pressure using a flow-circulation method under conditions when a reverse reaction can be ignored [40–47]. Varying the size of catalyst granules demonstrated that these reactions occur in a kinetic region on grains of size 0.25–0.1 mm. The rates of formation of individual products were expressed in moles of a corresponding carbon oxide or acetone consumed for the formation of these products in 1 s per 1 m^2 of the active metal surface. The specific surface area S_0 of a metal was calculated from the chemisorption of oxygen under pulsed chromatographic conditions; the average metal particle size d was determined from adsorption data according to the equation [48]

$$d = \frac{\beta}{S_0 \rho}, \quad (1)$$

where ρ is the density of particles, S_0 is the specific surface area of an active component, and β is a coefficient that takes into account the shape of particles. Tables 2–5 summarize kinetic and physicochemical parameters of supported catalysts.

The rate constant of reaction is determined by the Arrhenius function

$$k = k_0 e^{-\frac{E}{RT}}, \quad (2)$$

where k_0 is the preexponential factor, R is the gas constant, and T is temperature.

Using the transition state method as applied to surface reactions, the preexponential factor of the rate constant can be expressed by the equation

$$k_0 = \chi G L \frac{kT}{h} e^{\frac{\Delta S^*}{R}}, \quad (3)$$

where χ is the transmission coefficient, L is the number of surface elements per unit surface area of the catalyst, G is the number of possible positions of an activated complex, kT is the product of the Boltzmann constant and the temperature, h is the Planck constant, and ΔS^* is the activation entropy.

Results and Discussion

The activation entropy ΔS^* in the same reaction on a number of supported catalysts of different chemical nature is approximately constant [48] because the activated complexes are structurally similar. Consequently, differences in preexponential factors on various catalysts depend on a geometric factor. The probability of the occurrence of complex active centers on larger particles of an active component than that on small particles. Then, the value of L in Eq. (3) depends on a particle size distribution.

In the test catalysts, metal particles are randomly distributed on an inert support with a developed inner surface. Most frequently, the distribution of a highly dispersed component in real supported catalysts cannot be described by a standard curve [49, 50]; as a rule, the distribution function density is strongly asymmet-

Table 3. Physicochemical and catalytic properties of various catalysts in carbon dioxide hydrogenation [42, 43]

Entry	Catalyst	E_5, kJ/mol	$k_5 \times 10^7$, mol m^{-2} s^{-1}	d, nm
1	Ni/Al_2O_3	85	0.4	1.4
2	Pd/Al_2O_3	94	1.1	7.6
3	Rh/Al_2O_3	78	3.1	4.0
4	Rh/TiO_2	95	4.5	29.5
5	Rh/Nb_2O_5	90	16.0	19.5
6	Rh/ZrO_2	84	2.0	11.4
7	Rh/MgO	93	9.9	40.0

Table 4. Catalytic activity of Co and Ni particles on various supports in CO hydrogenation and the average sizes of these particles [44, 45]

Entry	Catalyst	E_{eff}, kJ/mol	$W \times 10^7$, mol m^{-2} s^{-1}	d, nm
		Cobalt		
1	BeO	87	5.5	18
2	Al_2O_3	74	4.3	6
3	SiO_2	114	52.0	38
4	Cr_2O_3	58	5.3	15
5	ZrO_2	98	8.4	33
6	MgO	24	1.0	3
		Nickel		
1	BeO	83	27	21
2	SiO_2	91	3.2	6
3	Cr_2O_3	84	1.9	12
4	ZrO_2	73	262	97
5	Al_2O_3	78	11.4	2.4

Note: Reaction mixture, $P_{CO} = 20$ kPa and $P_{H_2} = 50$ kPa.

Table 5. Catalytic activity of Ni particles on various supports in acetonitrile hydrogenation and the average sizes of these particles [46, 47]

Entry	Catalyst	E_{eff}, kJ/mol	$W \times 10^6$, mol m^{-2} s^{-1}	d, nm
1	BeO	39	9.4	21
2	MgO	23	4.6	1
3	SiO_2	26	1.53	6
4	WO_3	37	4.0	86.4
5	ZrO_2	31	33.4	98.7
6	Al_2O_3	41	1.0	2.4

ric. Therefore, we used the following density distribution function (Fig. 4) [51, 52]:

$$\varphi(r) = \alpha r^{-\mu}. \quad (4)$$

It allowed us to approximate the distribution of the major portion of an active component; in this case, the most probable value of r_m is close to the minimum size r_1. This distribution is characteristic of both particles and pores.

The particle sizes of the active component lie in some range. Consequently, the specific surface area of a system that consists of particles with a certain shape is equal to the sum of the surface areas of all of the particles, which is expressed by the following equation in extreme case:

$$S = f\int_{r_1}^{r_2}\varphi(r)r^2 dr, \quad (5)$$

where f is a coefficient depending on the shape and number of particles per unit weight of an active component; $\varphi(r)$ is the probability density of a particle size distribution; and r_1 and r_2 are the minimum and maximum linear dimensions of particles, respectively. The solution of this equation makes it possible to determine the dependence of the specific surface area of the dispersed substance on the average size d of its particles.

In a study of the activity of catalysts, the active specific surface area is used, which is calculated from data on the chemisorption of various substances (H_2, O_2, CO, etc.), which serve as probes. The value of S_0 thus found is the surface area measured with a probe with the linear size r_0 (the size of the adsorption complex of the probe). In turn, the rate of a catalytic reaction is a linear function of the number of active centers with the linear size r'. The preexponential factor of the rate constant of a reaction on catalysts of the same type is constant only in the case that the same activated complex is used as a probe. We denote this preexponential factor by $k_{0,r'}$. Tripol'skii and Strizhak [53] found that, if the particle size distribution of an active component is described by Eq. (4), the preexponential factor depends on the average particle size in the following manner:

$$\ln k_0 = A - BD_f = A - \frac{B}{1-\left(\frac{r_0}{r_m}\right)^{\mu-2}\frac{r_m}{d}}, \quad (6)$$

where $A = \ln k_{0,r'} + 2\ln\left(r'/r_0\right)$ and $B = \ln\left(r'/r_0\right)$.

Equation (6) characterizes the dependence of the logarithm of the preexponential factor on the average particle size of an active component found based on adsorption data. The logarithm of k_0 increases with d; graphically, this can be described as a saturation curve.

Let us analyze the resulting equations using the reaction of acetone hydrogenation as an example. The stepwise mechanism of this process, which is based on a detailed kinetic and adsorption study, includes the hydrogenation of adsorbed acetone by adsorbed H atoms as a rate-limiting step [40, 41].

(1) $(CH_3)_2CO + Z_A = Z_A(CH_3)_2CO$;

(2) $H_2 + 2Z_H = 2Z_HH$;

(3) $Z_A(CH_3)_2CO + Z_HH \longrightarrow Z_A(CH_3)_2COH + Z_H$;

(4) $Z_A(CH_3)_2COH + Z_HH \longrightarrow Z_H(CH_3)_2CHO + Z_A$;

(5) $Z_H(CH_3)_2CHOH \longrightarrow (CH_3)_2CHOH + Z_H$.

At the first two steps, an adsorption equilibrium between initial reactants is established. Hydrogen and acetone are adsorbed at Z_H and Z_A centers, respec-

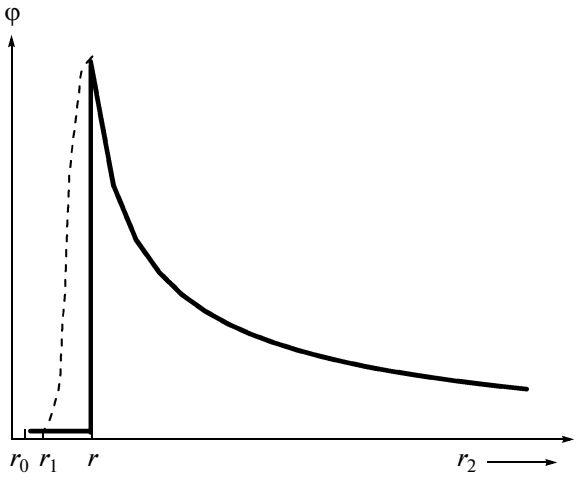

Fig. 4. Plot of the density distribution function of particles according to Eq. (4). The dashed line shows the real distribution of particles.

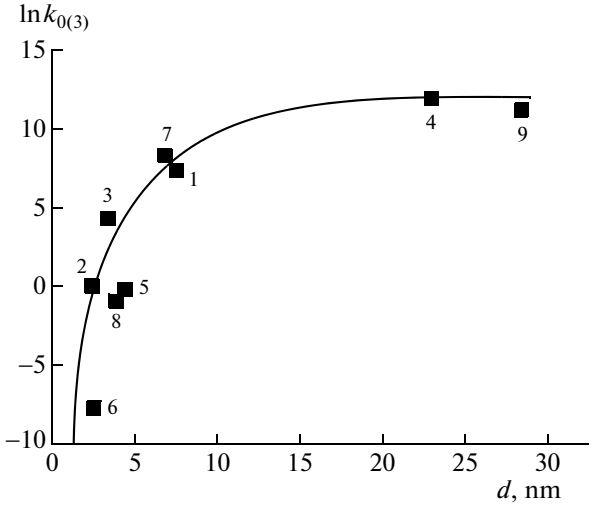

Fig. 5. Dependence of the logarithm of the preexponential factor of the rate constant of a rate-limiting step in acetone hydrogenation on the particle size of an active component of the catalyst. The numbers of catalysts are indicated in accordance with Table 2.

tively. The kinetics of alcohol formation is described by the equation [40, 41]

$$W = k_3\theta_A\theta_H = k_3\frac{b_A P_A}{1+b_A P_A}\frac{\sqrt{b_{H_2}P_{H_2}}}{1+\sqrt{b_{H_2}P_{H_2}}}, \qquad (7)$$

where k_3 is the rate constant of the third step; θ_A and θ_H are surface coverages with acetone and hydrogen, respectively; and b_i are adsorption coefficients.

From Table 2, it follows that the activation energies of the reaction on the test catalysts were different because E_a strongly depends on the chemical nature of a metal. However, the chemical nature of a catalyst affects only slightly the preexponential factor of the rate constant of the rate-limiting step. Equation (6) adequately describes (Fig. 5) the preexponential factors (Table 2).

Similar results were obtained in studies of the reaction of carbon dioxide hydrogenation [42, 43]. In this case, carbon monoxide can be formed along with hydrocarbons. Tripol'skii et al. [43] reported the complete mechanism of the reaction, which occurs via three paths. This mechanism describes the formation of all of the possible CO_2 hydrogenation products and includes more than 14 steps. However, almost 100% selectivity for methane formation was reached on catalysts given in Table 3. Thus, it is not necessary to analyze the entire mechanism, and it is sufficient to restrict ourselves by the consideration of the following first six steps:

(1) $H_2 + 2Z = 2ZH$,

(2) $CO_2 + 2ZH = Z_2CO_2H_2$,

(3) $Z_2CO_2H_2 + ZH = Z_2HCO_2H_2 + Z$,

(4) $Z_2HCO_2H_2 + ZH = Z_2H_2CO_2H_2 + Z$,

(5) $Z_2H_2CO_2H_2 \longrightarrow ZCHOH + H_2O + Z$,

(6) $ZCHOH + ZH \longrightarrow ZCH \xrightarrow{ZH} CH_4 + H_2O + Z$.

In the first four steps, an equilibrium is established. Carbon dioxide from a gas phase interacts with two adsorbed hydrogen atoms to form the intermediate complex $Z_2CO_2H_2$, and the consecutive addition of two hydrogen atoms to this complex results in $Z_2H_2CO_2H_2$. Upon the decomposition of this intermediate compound, ZCHOH is formed, and methane is the hydrogenation product of this substance. Step 5 is a rate-limiting step; consequently, the reaction proceeds through the formation of the same activated complex on all of the catalysts. According to the above mechanism, the rate of methane formation is described by the equation

$$W_{CH_4} = k_5K_2K_3K_4P_{CO_2}\left(b_{H_2}P_{H_2}\right)^2(\theta^0)^2, \qquad (8)$$

where k_5 is the rate of the rate-limiting step; K_i are the equilibrium constants of the corresponding steps; b_{H_2} is the adsorption coefficient of hydrogen; P_i are the partial pressures of reactants; and θ^0 is the fraction of a free catalyst surface.

Figure 6 shows the dependence of the logarithm of the preexponential factor of the rate constant of the rate-limiting step on the average particle size d of a transition metal. It follows that Eq. (6) adequately describes experimental data obtained upon the hydrogenation of carbon dioxide on all of the test catalysts.

An analogous approach can be used to analyze the kinetics of a catalytic reaction in the case that the numerical values of the rate constants of elementary steps are unknown. Let us consider the reaction of carbon monoxide hydrogenation [44, 45]. The stepwise

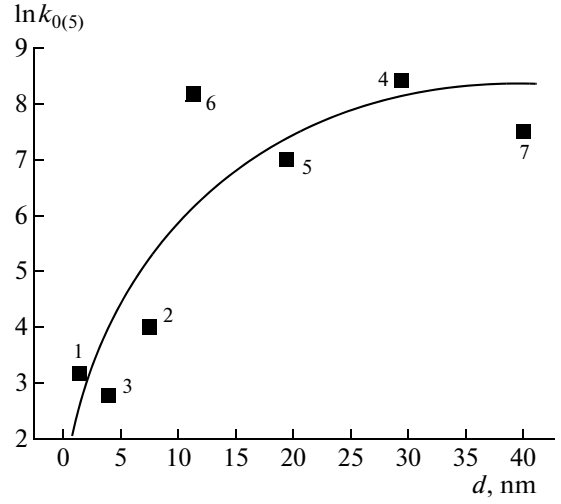

Fig. 6. Dependence of $\ln k_{0(5)}$ on the average size of metal particles in the reaction of carbon dioxide hydrogenation. The numbers of catalysts are indicated in accordance with Table 3.

mechanism of this process was proposed based on a detailed kinetic and adsorption study:

(1) $CO + Z = ZCO$;
(2) $H_2 + 2Z = 2ZH$;
(3) $ZCO + ZH = ZCOH + Z$;
(4) $ZCOH + ZH \longrightarrow ZX_0 + Z$;
(5) $ZX_0 + ZH \longrightarrow ZX_0' \xrightarrow{ZH} CH_4 + H_2O + Z$;
(6) $ZX_0 + ZX_0 \longrightarrow ZX_1 \xrightarrow{ZH} C_2H_6 + ... + Z$.

In steps 1–3, an adsorption equilibrium is established; the surface reaction between ZCOH and ZH (step 4) is a rate-limiting step. The above mechanism corresponds to the following equation for the overall rate of CO conversion:

$$W = k_4 \frac{K_3 b_{CO} P_{CO} b_{H_2} P_{H_2}}{\left[1 + b_{CO} P_{CO} + \sqrt{b_{H_2} P_{H_2}} + (1 + K_3 b_{CO} P_{CO})\right]^2}, \quad (9)$$

where k_4 is the rate constant of the rate-limiting step; K_3 is the equilibrium constant of the third step; and b_i are adsorption coefficients.

Table 4 summarizes the specific rates of reaction on Co and Ni particles on various supports at the same reaction mixture composition. The specific rate is proportional to the effective rate constant, which, in turn, is the product of the rate constant of a rate-limiting step and the equilibrium constants of fast reversible steps of the process. With consideration for Eq. (9), the rate of a catalytic reaction can be described by the expression

$$W \propto k_{eff} = k_{eff}^0 \exp\left(E_{eff}/RT\right) \propto k_4 K_3 b_{CO} b_{H_2}, \quad (10)$$

where k_{eff} is the effective rate constant, and E_{eff} is the effective activation energy, which includes the activation energy of the rate-limiting step 4, the enthalpy of the third step, and the heats of adsorption of the initial substances.

On the other hand,

$$W_0 \propto k_{eff}^0 = k_4^0 K_3^0 b_{CO}^0 b_{H_2}^0 = k_4^0 e^{-\frac{\Delta S_4 + \Delta S_{CO} + \Delta S_{H_2}}{R}}, \quad (11)$$

where ΔS_i is the entropy change in steps 1–3. The above assumption that the entropy of activation of an activated complex is constant for the same reaction on various catalysts [48] is also fully true of entropy changes in these steps. In this case, the preexponential factor of the rate constant k_0 in Eq. (6) may be replaced by W_0. Thus, we obtain

$$\ln W_0 = A - \frac{B}{1 - \left(\frac{r_0}{r_m}\right)^{D_f - 2} \frac{r_m}{d}}. \quad (12)$$

From Fig. 7, which shows the dependence of the logarithm of W_0 in the reaction of CO hydrogenation on the average size of cobalt and nickel particles on various supports, it follows that Eq. (12) adequately describes experimental data obtained in the hydrogenation of carbon monoxide on cobalt and nickel catalysts.

The results of the study of the kinetics of hydrogenation of acetonitrile on supported metal catalysts also support the above approach to the analysis of the dependence of rate constant on the particle size distribution of an active component. The complete mechanism of this process, which consists of three reaction paths and includes more than 13 steps, was published earlier [46, 47]. To analyze this mechanism, it is sufficient to restrict ourselves by the following first three steps:

(1) $CH_3CN + Z_N = Z_NCH_3CN$;
(2) $H_2 + 2Z_H = 2Z_HH$;
(3) $Z_NCH_3CN + Z_HH \longrightarrow Z_NCH_3CNH + Z_H$.

In steps 1 and 2, an adsorption equilibrium is established. The rate of reaction depends on the step of the interaction of adsorbed hydrogen atoms and acetonitrile. This mechanism corresponds to the following equation for the overall rate of acetonitrile conversion [46, 47]:

$$W = k_3 \theta_{CN} \theta_H, \quad (13)$$

where k_3 is the rate constant of the rate-limiting step, and θ_{CN} and θ_H are surface coverages with acetonitrile and hydrogen, respectively.

Table 5 summarizes the specific overall rates of reaction on Ni particles on various supports at the same reaction mixture composition. In this case, the values of θ_{CN} and θ_H are approximately constant, and the specific rate is proportional to the constant k_3:

$$W \propto k_3. \quad (14)$$

Figure 8 shows the dependence of the logarithm of W_0 on the average particle size of nickel on various

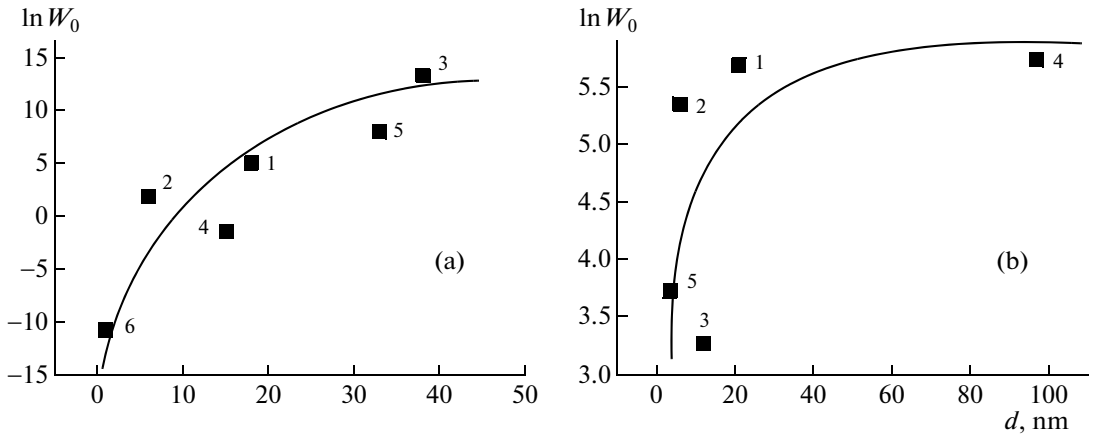

Fig. 7. Dependence of $\ln W_0$ on the average size of (a) cobalt or (b) nickel particles in the reaction of carbon monoxide hydrogenation. The numbers of catalysts are indicated in accordance with Table 4.

supports in the reaction of acetonitrile hydrogenation. As can be seen, Eq. (6) adequately describes experimental data obtained upon the hydrogenation of acetonitrile on nickel catalysts.

Thus, the approach proposed for describing the structure of supported catalysts allowed us to interpret and quantitatively express the frequently observed dependence of catalytic activity on the geometry of the active surface. Moreover, the occurrence of these dependences on different metals suggests that hydrogenation reactions proceed through the same activated complexes in all cases.

The use of the resulting dependences for the analysis of kinetic parameters of so-called structure-sensitive reactions opens up new opportunities for the technological design of optimum catalysts for various industrially important heterogeneous catalytic processes, in particular, the preparation of synthetic liquid fuel from carbon oxides.

Thus, the above study indicates that it is incorrect to consider the mechanism of the local interaction of adsorbed molecules with a catalyst surface from the standpoint of the separate effects of electronic and geometric factors. These factors are interrelated, and they equally affect the activity of heterogeneous catalysts. The electronic factor mainly manifests itself in the course of reaction on small particles (<10 nm), on which electron transition energies in an activated complex are size-dependent. Another reason for the effect of the electronic factor on the catalytic behavior of nanoparticles is that not only the fraction of surface atoms increases but also the ratio between atoms arranged at lattice faces, edges, and sites changes as the particle size is decreased; these atoms exhibit various coordinative unsaturation and, correspondingly, differ from each other in electronic properties. Above the specified limit (10 nm), only the geometry of active component nanoparticles exerts the main effect on catalytic properties. In this case, the role of the geometric factor depends on the accessibility of the active surface to reactants. If a catalytic process takes place at complex active centers including several surface atoms, the probability of the occurrence of these centers increases as the particles of an active component of the catalyst become larger. Consequently, the fraction of the active surface increases to reach saturation. Because real heterogeneous catalysts are polydisperse systems (i.e., they are characterized by a nanoparticle size distribution of the active component), their catalytic properties depend on both electronic and geometric factors, and the ratio between the contributions of these factors depends on the distribution function of active component particles. We can state that the division into electronic and geometric factors is tentative because both of them depend on the particle size and, consequently, geometry of the active component. Therefore, in the course of structure-sensitive hetero-

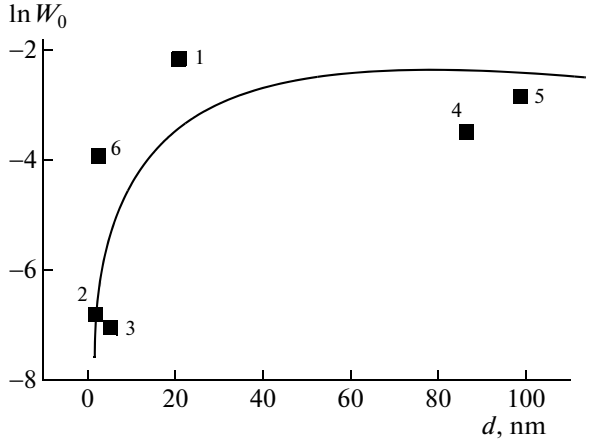

Fig. 8. Dependence of $\ln W_0$ on the average size of nickel particles in the reaction of acetonitrile hydrogenation. The numbers of catalysts are indicated in accordance with Table 5.

geneous catalytic reactions, the geometry and the chemical nature of the active component often have equally strong effects on the catalytic properties of the catalyst.

REFERENCES

1. Boreskov, G.K., *Geterogennyi kataliz* (Hetyerogeneous Catalysis), Moscow: Nauka, 1988.
2. Roginskii, S.Z., *Geterogennyi kataliz: Nekotorye voprosy teorii* (Heterogeneous Catalysis: Some Theoretical Topics), Moscow: Nauka, 1979.
3. Kobozev, N.I., *Zh. Fiz. Khim.*, 1939, vol. 13, p. 1.
4. Kobozev, N.I., *Zh. Fiz. Khim.*, 1940, vol. 14, p. 663.
5. Bond, G.C., *Surf. Sci.*, 1985, vol. 156, p. 966.
6. Bond, G.C., *Catal. Rev.*, 2008, vol. 50, p. 532.
7. Bukhtiyarov, V.I. and Slin'ko, M.G., *Usp. Khim.*, 2001, vol. 70, p. 167.
8. Bukhtiyarov, V.I., *Usp. Khim.*, 2007, vol. 76, p. 596.
9. Boudart, M., *Adv. Catal.*, 1969, vol. 20, p. 153.
10. Che, M. and Bennett, C.O., *Adv. Catal.*, 1978, vol. 36, p. 55.
11. Zhdanov, V.P. and Kasemo, B., *Surf. Sci. Rep.*, 2000, vol. 39, p. 25.
12. Boudart, M., *Chem. Rev.*, 1995, vol. 95, p. 661.
13. Narayanan, R. and El-Sayed, M.A., *Top. Catal.*, 2008, vol. 47, p. 15.
14. Rand, D.A.J. and Woods, R., *Surf. Sci.*, 1974, vol. 41, p. 611.
15. Haruta, M., *Catal. Today*, 1997, vol. 36, p. 153.
16. Bamwenda, G.R., Tsubota, S., Nakamura, T., and Haruta, M., *Catal. Lett.*, 1997, vol. 44, p. 83.
17. Haruta, M., *J. New Mater. Electrochem. Syst.*, 2004, vol. 7, p. 163.
18. Remediakis, I.N., Lopez, N., and Nørskov, J.K., *Appl. Catal., A*, 2005, vol. 291, p. 13.
19. Guczi, L., Horváth, D., Pászti, Z., and Petõ, G., *Catal. Today*, 2002, vol. 72, p. 101.
20. Hutchings, G.J., *Catal. Today*, 2005, vol. 100, p. 55.
21. Andersson, M.P., Abild-Pedersen, F., Remediakis, I.N., Bligaard, T., Jones, G., Engbæk, J., Lytken, O., Horch, S., Nielsen, J.H., Sehested, J., Rostrup-Nielsen, J.R., Nørskov, J.K., and Chorkendorff, I., *J. Catal.*, 2008, vol. 255, p. 6.
22. Lopez, N., Janssens, T.V.W., Clausen, B.S., Xu, Y., Mavrikakis, M., Bligaard, T., and Norskov, J.K., *J. Catal.*, 2004, vol. 223, p. 232.
23. Valden, M., Lai, X., and Goodman, D.W., *Science*, 1998, vol. 281, p. 1647.
24. Chen, M.S. and Goodman, D.W., *Catal. Today,* 2006, vol. 111, p. 22.
25. Goodman, D.W., *J. Catal.,* 2003, vol. 216, p. 213.
26. Heiz, U. and Schneider, W.-D., *J. Phys. D: Appl. Phys.*, 2000, vol. 33, p. R85.
27. Sykes, E.C.H., Tikhov, M.S., and Lambert, R.M., *Catal. Lett.,* 2002, vol. 82, p. 169.
28. Carnes, C.L. and Klabunde, K.J., *J. Mol. Catal.*, 2003, vol. 194, p. 227.
29. Chen, K., Bell, A.T., and Iglesia, E., *J. Catal.,* 2002, vol. 209, p. 35.
30. Li, P., Miser, D.E., Rabiei, S., Yadav, R.T., and Hajaligol, M.R., *Appl. Catal., B*, 2003, vol. 43, p. 151.
31. Nagase, K., Zheng, Y., Kodama, Y., and Kakuta, J., *J. Catal.,* 1999, vol. 187, p. 123.
32. Zheng, X., Wang, S., Zhang, S., Wang, S., Huang, W., and Wu, S., *React. Kinet. Catal. Lett.*, 2005, vol. 84, p. 29.
33. Koch, U., Fojtik, A., Weller, H., and Henglein, A., *Chem. Phys. Lett.*, 1985, vol. 122, p. 507.
34. Kim, S.Y., Yeon, Y.S., Park, S.M., Kim, J.H., and Song, J.K., *Chem. Phys. Lett.*, 2008, vol. 462, p. 100.
35. Strizhak, P.E., Didenko, O.Z., and Kosmambetova, G.R., *Mater. Lett.,* 2008, vol. 62, p. 4094.
36. Bahnemann, D.W., *Isr. J. Chem.*, 1993, vol. 33, p. 115.
37. Bahnemann, D.W., Kormann, C., and Hoffmann, M.R., *J. Phys. Chem.*, 1987, vol. 91, p. 3789.
38. Didenko, O.Z., Kosmambetova, G.R., and Strizhak, P.E., *Chin. J. Catal.*, 2008, vol. 29, p. 1079.
39. Meulenkamp, E.A., *J. Phys. Chem. B*, 1998, vol. 102, p. 5566.
40. Pavlenko, N.V., Tripol'skii, A.I., and Golodets, G.I., *Teor. Eksp. Khim.,* 1986, vol. 22, p. 698.
41. Pavlenko, N.V., Tripol'skii, A.I., Golodets, G.I., and Tel'biz, G.M., *Kinet. Katal.,* 1985, vol. 26, p. 115.
42. Tripol'skii, A.I., Odnovolik, V.I., and Pavlenko, N.V., *Teor. Eksp. Khim.*, 1996, vol. 32, p. 107.
43. Tripol'skii, A.I., Pavlenko, N.V., and Odnovolik, V.I., *Teor. Eksp. Khim.*, 1996, vol. 32, p. 134.
44. Pavlenko, N.V., Prokhorenko, E.V., Tripol'skii, A.I., and Golodets, G.I., *Kinet. Katal.,* 1989, vol. 30, p. 1364.
45. Pavlenko, N.V., Tripol'skii, A.I., Popovich, O.G., and Golodets, G.I., *Kinet. Katal.,* 1989, vol. 30, p. 848.
46. Pavlenko, N.V., Prokhorenko, E.V., and Golodets, G.I., *Kinet. Katal.,* 1987, vol. 28, p. 1382.
47. Pavlenko, N.V. and Golodets, G.I., *Neftepererab. Neftekhim.*, 1989, vol. 37, p. 1.
48. Golodets, G.I., *Geterogenno-kataliticheskie reaktsii s uchastiem molekulyarnogo kisloroda* (Heterogeneous-Catalytic Reactions Involving Molecular Oxygen), Kiev: Naukova Dumka, 1977.
49. Fenelonov, V.B., *Vvedenie v fizicheskuyu khimiyu formirovaniya supramolekulyarnoi struktury adsorbentov i katalizatorov* (Introduction to the Physical Chemistry of the Formation of Supramolecular Structures of Adsorbents and Catalysts), Novosibirsk: Sib. Otd. Ross. Akad. Nauk, 2004.
50. Brilliantov, N.V., Andrienko, Yu.A., and Krapivsky, P.L., *Physica A,* 1997, vol. 239, p. 267.
51. Neimark, A.V., *Zh. Fiz. Khim.*, 1990, vol. 64, p. 2593.
52. Kukushkin, S.A. and Slizov, V.V., *Dispersnye sistemy na poverkhnosti tverdykh tel: mekhanizmy obrazovaniya tonkikh plenok (evolyutsionnyi podkhod)* (Disperse Systems on Solid Surfaces: Thin Film Formation Mechanisms (Evolutionary Approach)), St. Petersburg: Nauka, 1996.
53. Tripol'skii, A.I. and Strizhak, P.E., *Teor. Eksp. Khim.*, 2007, vol. 43, p. 102.